Acta Urol. Jap. Vol. 23, No. 7
September-October 1977

ELEMENTAL ANALYSIS OF URINARY TRACT CALCULI WITH ELECTRON MICROSCOPE HAVING AN ELECTRON PROBE X-RAY MICROANALYZER

Fumitaka KENNOKI*

From the Department of Urology, Nippon Medical School

The simultaneous elemental analysis of a small area of an urinary tract calculi and observation of its surface and nucleus was attempted with a conventional transmission electron microscope fitted with a scanning device, side-entry goniometer stage and an energy dispersive type X-ray microanalyzer unit, and coupled to a computer system.

The experimental results obtained with three different types of calculi, as determined by X-ray diffraction, derived from six patients are given below.

In three samples of apatite calculus: Calcium (Ca) and phosphorus (P) were detected in all samples but magnesium (Mg) was observed in one case. A count was made of the energy intensity ratio between Ca and P in the three samples and a control sample of hydroxyl apatite $Ca_{10}(PO_4)_6(OH)_2$. None of the counts coincided.

In one sample of whewellite calculus: P was detected in the nucleus in addition to Ca.

In two samples of cystine calculus: Ca and P were detected in addition to sulfur (S).

These results indicated that calculi do not always consist of a single substance, and that the crystal structure of apatite in calculi is of an immature form in comparison with that of the hydroxyl apatite control sample.

INTRODUCTION

Determination of the chemical composition of urinary tract calculi has been widely carried out by means of one or the other of the following methods: crystallography and X-ray diffraction (Prien and Frondel, 1947; Prien, 1963; Sutor and Scheidt, 1968; Sutor et al., 1974), chemical analysis (La Towsky, 1943; Hodgkinson et al., 1969; Westbury and Omenogor, 1970; Westbury, 1974), infrared spectroscopy (Beischer, 1955; Takasaki, 1975) and electron diffraction (Meyer et al., 1971).

In regard to elemental analysis of a small area of a calculus, Chambers et al. (1972) used an electron probe X-ray microanalyzer of the wavelength dispersive type. In this system, the individual elements are detected through their known wavelengths.

Mizuhira (1976) utilized the energy dispersive type instead of the wavelength dispersive type for elemental analysis of biological specimens. In this system, the energy of X-ray pulses from elements ranging between sodium (Na) and uranium (U) is detected simultaneously, and therefore almost all kinds of elements present can be detected through the determination of the position of their individual energy peaks.

The energy dispersive type of X-ray microanalyzer has the following advantages:

1. The ratio of the energy intensity between several elements can be measured, and each weight fraction assumed. It therefore follows that the elemental molecular formulation can be understood.
2. A clear electron scanning image can also be observed in addition to the analysis.
3. It is easy to use.

Therefore we applied the energy disper-

* 100 Sendagi 1-1-5 Bunkyo-ku, Tokyo, Japan

sive type X-ray microanalyzer plus computer system in our attempts to analyze the elements in a small area of urinary tract calculi.

MATERIALS AND METHODS

The subjects were six patients with urolithiasis whose calculi had been surgically removed and classified, by the X-ray diffraction method (Table 1), into apatite, whewellite and cystine calculi.

The calculi were washed for one hour in several changes of distilled water in order to remove extraneous blood and tissue, and then dried at room temperature. Specimens were taken from either the nuclei or surfaces of the calculi. Controls used were hydroxyl apatite $Ca_{10}(PO_4)_6(OH)_2$ (Seikagaku Kogyo, Tokyo), whewellite $CaC_2O_4H_2O$ (Koso Chemical Co., Ltd., Tokyo) and *L*-cystine $[-SCH_2CH(NH_2)COOH]_2$ (Nippon Rikagakuyakuhin K.K.).

Table 1. Details of stones from patients.

Patients No.	Sex	Type of stone	Area	Composition (by X-ray diffraction)
1	F	Kidney	Nucleus	Apatite
2	M	Kidney	Nucleus	Apatite
3	M	Kidney	Surface	Apatite
4	M	Ureter	Nucleus	Whewellite
5	F	Kidney	Surface	Cystine + (Apatite)
6	M	Ureter	Nucleus	Cystine

A minute quantity of each calculi and control material was ground with an agate grinder. Ground fine powder of each sample was suspended in deionized water. A small droplet of suspension was mounted on a carbon plate with a micropippet and dried. The sample-mounted carbon plate was then coated with carbon. The carbon plates for X-ray microanalysis were made from carbon rods using a dental engine, and their surface smoothed with a grinder(Mizuhira 1976).

Observation and analysis was carried out with a JEM 100-C transmission electron microscope fitted with a scanning device (ASID-4), side-entry goniometer stage (SEG), and energy dispersive type X-ray microanalyzing unit (EDAX-707B), and a computer system (EDIT). The accelerating voltage for X-ray excitation was 20 KeV. The specimen illuminating current was 5×10^{-10} A, and the scanning time 100 or 200 seconds.

Surface images of calculi were obtained by secondary electron scanning with a conventional transmission electron microscope. Elements in each calculi and control material were then identified by both scanning and line analyzing X-ray pulses.

Small background waves of static were removed from the spectrum of scanning X-ray pulses by manual stripping, individual peaks were counted, and then the ratio of energy intensity between the several elements was calculated by manual thin section in the computer system.

RESULTS

Apatite calculi

Case 1.

Secondary electron image: Individual plaques on the radius plane of the nucleus of the apatite calculus were unequal in size (approx. 2～5 μm), and the several clumps of plaques also were unequal in size (Fig. 1).

X-ray analysis: When X-ray pulses from some part of the same surface observed by secondary electron image were scanned, there were three peaks in the energy spectrum together with small background waves. The latter were removed by automatic stripping in the computer system, and the spectrum became clear (Fig. 1, lower). Two of the peaks were easily identified as Ca-Kα and Ca-Kβ

energy. The third peak was identified, by manual stripping in the computer system, as P-Kα and P-Kβ. Manual thin section in the computer system revealed the ratios of energy intensities of Ca-Kα, Ca-Kβ, P-Kα and P-Kβ to be 1.0000 : 0.5791 : 0.6885 : 0.2069 (Table 2).

When X-ray pulses of Ca-Kα and P-Kα along the middle of the same surface area observed by secondary electron image were line analyzed, they were seen to have a similar movement (Fig. 1). In other words, there was a similar distribution of both elements.

Case 2.

Secondary electron image: The surface of the calculus had many small indentations and many fissures. The latter were in an approximately parallel row, and were either deep or very shallow (Fig. 2).

X-ray analysis: The energy spectrum had three peaks similar to Case 1 (Fig. 2 lower). The energy of Ca-Kα, Ca-Kβ, P-Kα and P-Kβ was counted. The ratios of energy intensities of Ca-Kα, Ca-Kβ, P-Kα and P-Kβ were 1.0000 : 0.6500 : 0.5291 : 0.5440 (Table 2).

Line analysis of Ca-Kα and P-Kα along the middle of the same surface area showed them to have dissimilar movement (Fig. 2).

Case 3.

Secondary electron image: Particles of various shapes and sizes were scattered on the surface of the calculus. Some were observed to have prong-like projections (Fig. 3).

X-ray analysis: Unlike Case 1 and 2, the energy spectrum demonstrated four peaks (Fig. 3 lower). Two of these peaks were easily identified as Ca-Kα and Ca-Kβ. P-Kα, P-Kβ, Mg-Kα and Mg-Kβ values could be counted from the other two peaks. The ratios of energy intensities of Ca-Kα, Ca-Kβ, P-Kα, P-Kβ, Mg-Kα and Mg-Kβ were 1.0000: 0.6070: 0.5734: 0.5783: 0.0535: 0.0538(Table 2).

Line analysis of Ca-Kα, P-Kα and Mg-Kα along the middle of the same surface area showed all three to have similar movement (Fig. 3).

Whewellite calculi

Case 4.

Secondary electron image: The radius plane of the nucleus was smooth with cracks in some places (Fig. 4).

Table 2. Energy counts and energy intensity ratios obtained with EDAX 707B-EDIT computer system.

Case 1

Elements	Energy counts	Ratio of energy intensity
Ca Kα	9724	1.0000
Ca Kβ	1128	0.5791
P Kα	5273	0.6885
P Kβ	317	0.2069

(20 KeV. 5×10^{-10}A. 100 Sec.)

Case 2

Elements	Energy counts	Ratio of energy intensity
Ca Kα	9538	1.0000
Ca Kβ	1034	0.6500
P Kα	5507	0.5291
P Kβ	295	0.5440

(20 KeV. 5×10^{-10}A. 100 Sec.)

Case 3

Elements	Energy counts	Ratio of energy intensity
Ca Kα	12274	1.0000
Ca Kβ	1476	0.6070
P Kα	4687	0.5734
P Kβ	3189	0.5783
Mg Kα	418	0.0535
Mg Kβ	372	0.0538

(20 KeV. 5×10^{-10}A. 100 Sec.)

Case 4

Elements	Energy counts	Ratio of energy intensity
Ca Kα	14292	1.0000
Ca Kβ	1623	0.5677
P Kα	202	0.0179
P Kβ	19	0.0084

(20 KeV. 5×10^{-10}A. 200 Sec.)

Case 5

Elements	Energy counts	Ratio of energy intensity
S Kα	10820	1.0000
S Kβ	2036	0.0641
Ca Kα	2037	0.1721
Ca Kβ	153	0.0248
P Kα	311	0.0581
P Kβ	62	0.0353

(20 KeV. 5×10^{-10}A. 100 Sec.)

Case 6

Elements	Energy counts	Ratio of energy intensity
S Kα	10490	1.0000
S Kβ	122	0.0581
Ca Kα	3635	0.3516
Ca Kβ	345	0.1668
P Kα	3454	0.3502
P Kβ	697	0.3533

(20 KeV. 5×10^{-10}A. 100 Sec.)

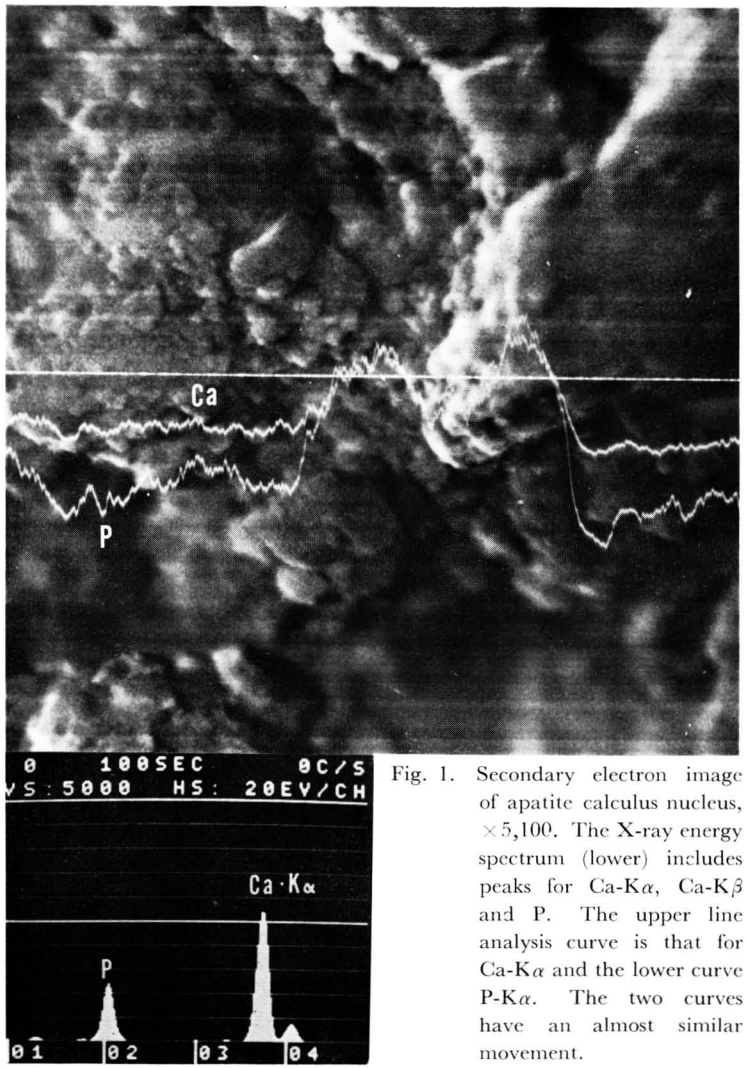

Fig. 1. Secondary electron image of apatite calculus nucleus, ×5,100. The X-ray energy spectrum (lower) includes peaks for Ca-Kα, Ca-Kβ and P. The upper line analysis curve is that for Ca-Kα and the lower curve P-Kα. The two curves have an almost similar movement.

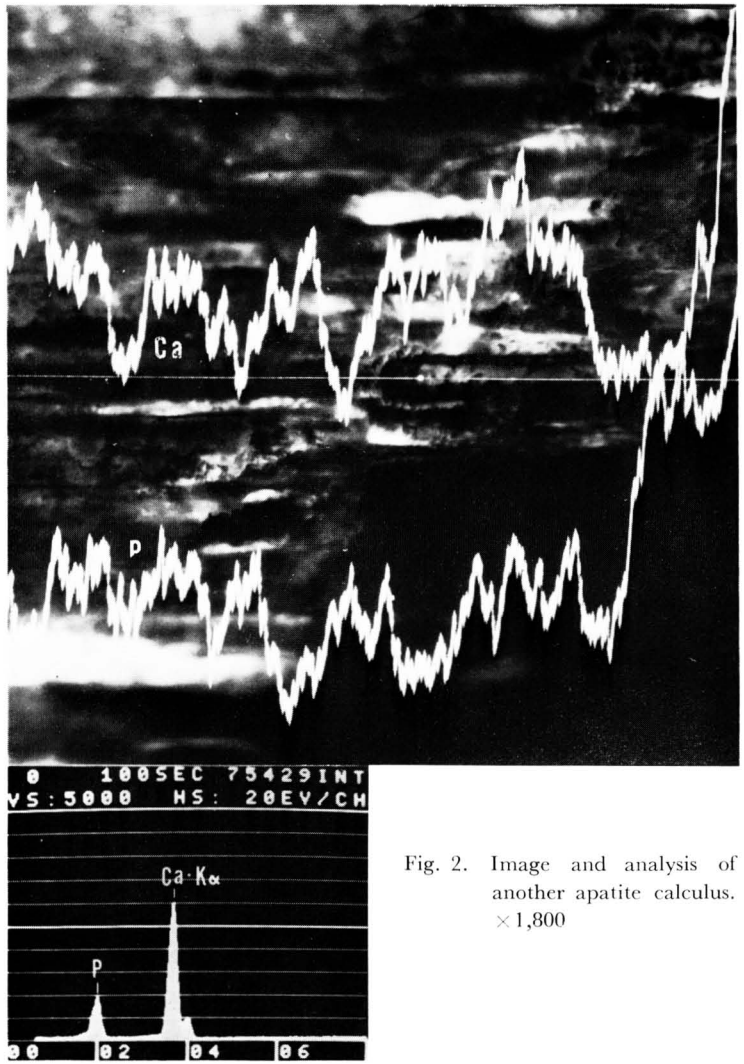

Fig. 2. Image and analysis of another apatite calculus. ×1,800

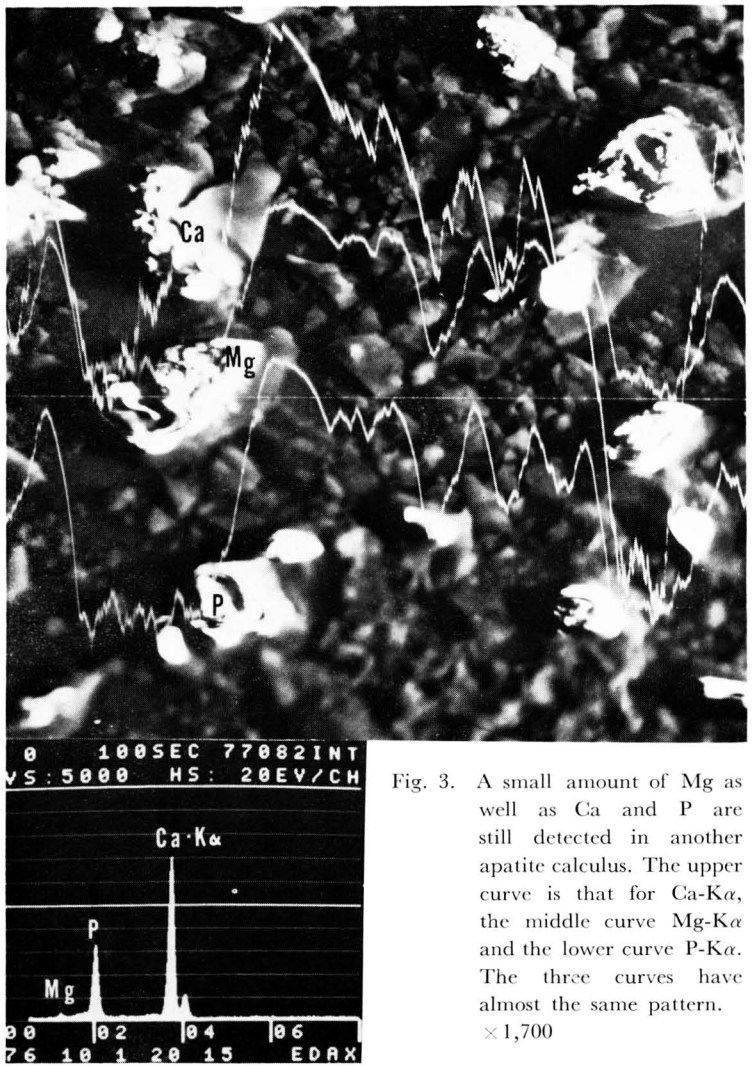

Fig. 3. A small amount of Mg as well as Ca and P are still detected in another apatite calculus. The upper curve is that for Ca-Kα, the middle curve Mg-Kα and the lower curve P-Kα. The three curves have almost the same pattern. $\times$1,700

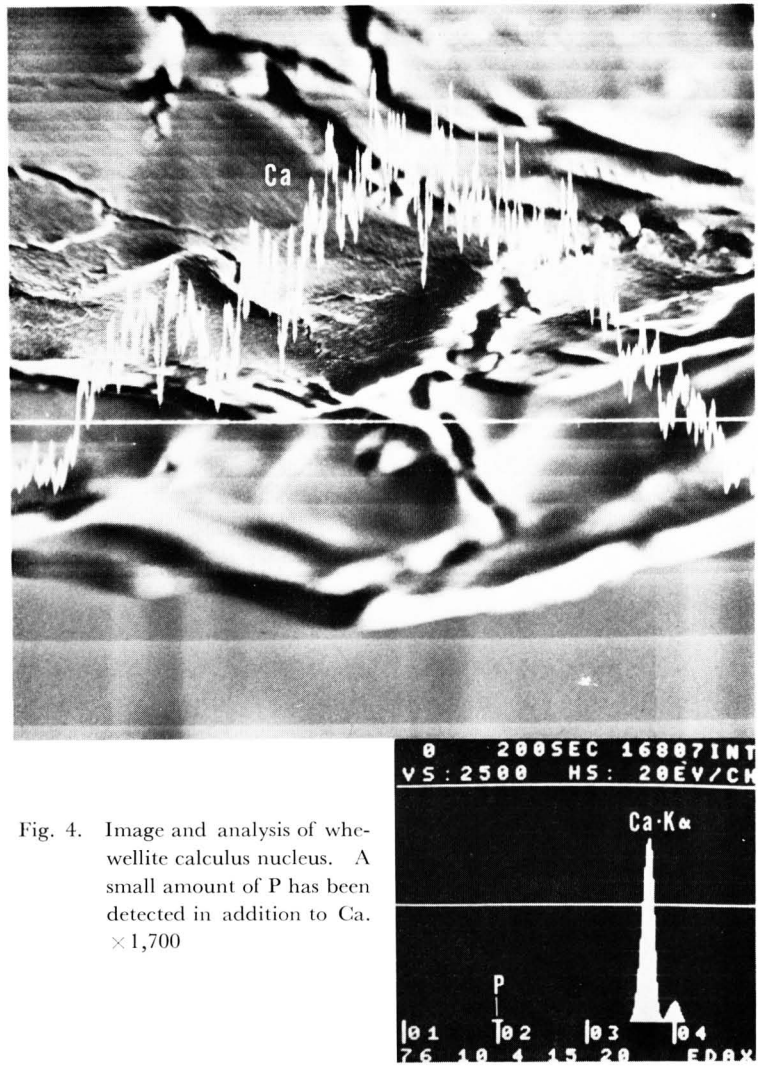

Fig. 4. Image and analysis of whewellite calculus nucleus. A small amount of P has been detected in addition to Ca. $\times$1,700

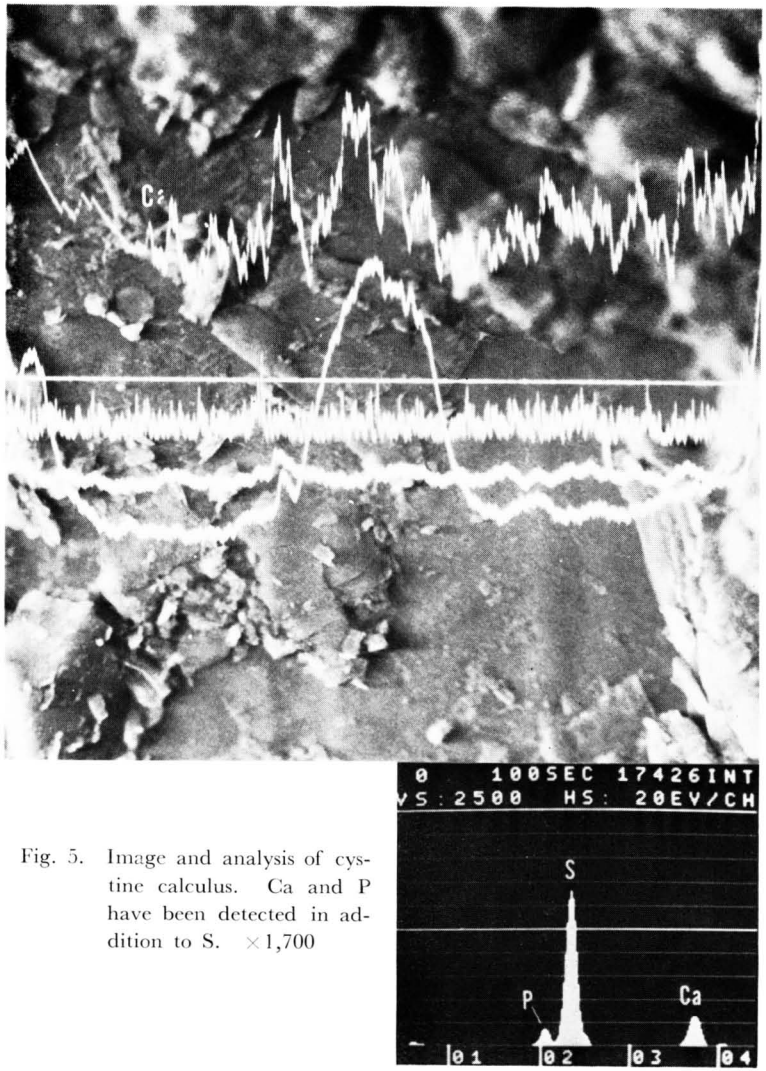

Fig. 5. Image and analysis of cystine calculus. Ca and P have been detected in addition to S. ×1,700

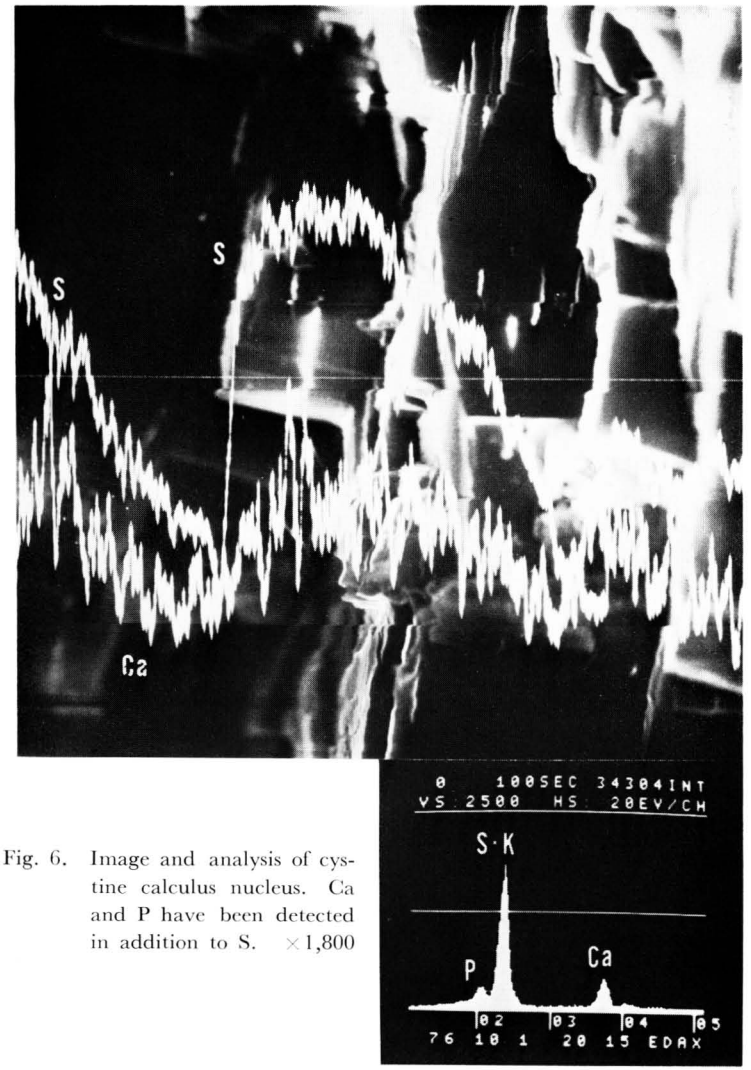

Fig. 6. Image and analysis of cystine calculus nucleus. Ca and P have been detected in addition to S. ×1,800

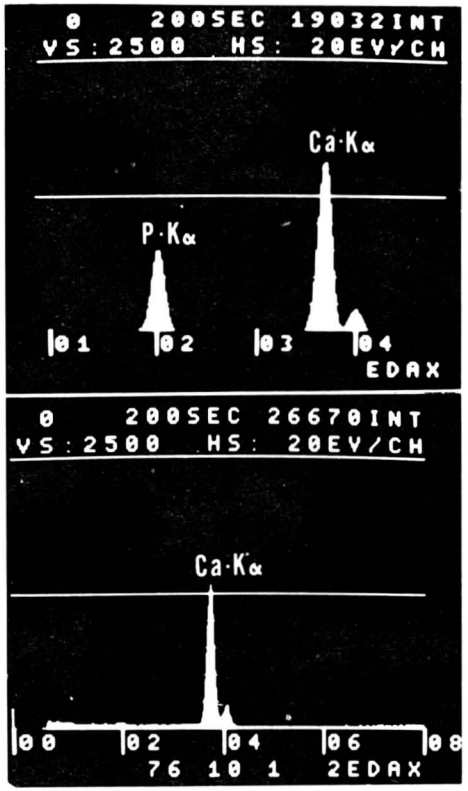

g. 7. Ca and P are detected in the control apatite (upper) and only Ca is detected in the control whewellite.

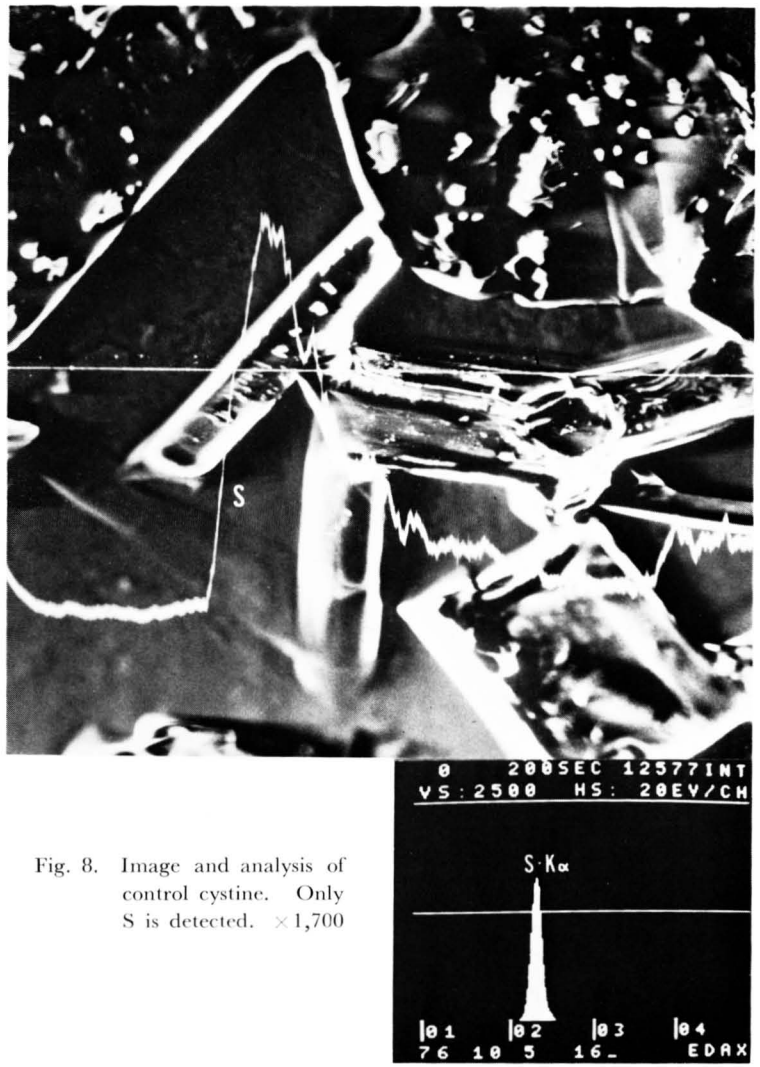

Fig. 8. Image and analysis of control cystine. Only S is detected. ×1,700

X-ray analysis: The energy spectrum had three peaks (Fig. 4 lower). Two peaks were easily identified as Ca-Kα and Ca-Kβ, while energy counts of P-Kα and P-Kβ in the third peak were weak (Table 2).

Line analysis of Ca-Kα and P-Kα along the middle of the same surface area resulted in the obtaining of Ca-Kα waves but not P-Kα waves due to the low energy (Fig. 4).

Cystine calculi

Case 5.

Secondary electron image: There were thin tetragonal-shaped splinters on the surface of the calculus, while several fine particles were seen scattered here and there (Fig. 5).

X-ray analysis: The energy spectrum had four peaks (Fig. 5 lower). Two were easily identified as Ca-Kα and Ca-Kβ, while P-Kα and P-Kβ and S-Kα and S-Kβ could be counted in the other two peaks, respectively (Table 2).

Line analysis of Ca-Kα, P-Kα and S-Kα along the middle of the same surface area revealed an even distribution of Ca-Kα and P-Kα but hardly any S-Kα (Fig. 5).

Case 6.

Secondary electron image: Square and hexagonal pillar-like crystals were observed on the radius plane of the nucleus of the calculus. These crystals were arranged close to each other (Fig. 6).

X-ray analysis: The energy spectrum had four peaks (Fig. 6 lower), from which Ca-Kα and Ca-Kβ, P-Kα and P-Kβ, and S-Kα and S-Kβ could be counted (Table 2).

Line analysis of S-Kα and Ca-Kα along the middle of the same surface area revealed the two elements to be distributed inalmost the same area (Fig. 6).

Control experiments

Hydroxyl apatite

The secondary electron image could not be obtained, nor line analysis carried out due to static.

X-ray analysis: The spectrum obtained had a similar pattern to that for apatite calculi but without an Mg peak (Fig. 7 upper). Ca-Kα, Ca-Kβ, P-Kα and P-Kβ counts were substantial. The ratios of energy intensities of Ca-Kα, Ca-Kβ, P-Kα and P-Kβ were 1.0000 : 0.6007 : 0.4575 : 0.3275 (Table 3).

Table 3. Energy counts and energy intensity ratios obtained with EDAX 707B-EDIT computer system.

Apatite control

Elements	Energy counts	Ratio of energy intensity
Ca Kα	11502	1.0000
Ca Kβ	1382	0.6007
P Kα	4947	0.4575
P Kβ	1382	0.3275

(20 KeV. 5×10^{-10}A. 200 Sec.)

Whewellite control

Elements	Energy counts	Ratio of energy intensity
Ca Kα	7520	1.0000
Ca Kβ	779	0.5179

(20 KeV. 5×10^{-10}A. 200 Sec.)

Cystine control

Elements	Energy counts	Ratio of energy intensity
S Kα	11209	1.0000
S Kβ	319	0.1422

(20 KeV. 5×10^{-10}A. 200 Sec.)

Whewellite

As in the case of hydroxyl apatite, the secondary electron image could not be obtained or line analysis carried out because of static.

X-ray analysis: The two peaks in the spectrum were Ca-Kα and Ca-Kβ (Fig. 7 lower). Ca-Kα and Ca-Kβ counts were substantial (Table 3).

L-Cystine

Secondary electron image: Tetragonal crystals of various sizes were observed. They were like transparent pieces of glass, with sides about 20 μm long (Fig. 8).

X-ray analysis: The spectrum had one peak (Fig. 8, lower), and S-Kα and S-Kβ could be counted (Table 3).

DISCUSSION

Urinary tract calculi, whether apatite, whewellite or cystine, are known to contain such light elements as Ca, P, S, etc. The characteristic X-ray energy of each of these elements was less than 8 KeV, and so there was no overlapping of their peaks .This means that an energy dispersive type X-ray microanalyzer can indicate

the cha racteristic elemental composition of any part of a calculus.

In X-ray microanalysis of a calculus, findings can differ in relation to differences in the direction, angle, length and absorption of the electron beam. Therefore, in order to make them as flat and thin as possible, both calculi and control samples were ground to a fine powder with an agate grinder. The powder was suspended in deionized water. A small drop of this suspension was mounted on a carbon plate with a micropipet. Carbon plates were utilized in order to avoid white X-ray noise.

In order to ensure accuracy in our findings, values were repeatedly determined and the average was used as the end result. *Apatite calculi*

It is natural that Ca and P were detected in apatite calculi, but Mg was also detected in one case. X-ray diffraction did not suggest that the Mg was present in the calculus in the form of a chemical compound of Mg. This means that an energy dispersive type microanalyzer is superior to elemental analysis in small areas of calculi.

The energy intensity ratios of Ca and P for the apatite control and the three calculi were all different. Duncumb (1968) and Russ (1974) have stated that energy intensity ratios are dependent on the weight fractions, in which case the ratio of Ca to P would be Ca-Kα: P-Kα. It therefore follows that the weight fractions of Ca and P were all different in the three calculi and the control, indicating that the compositions of the three calculi differed from that of the control apatite crystal, the energy intensity ratio of which was 20 : 9. It therefore can be concluded that the structure of apatite calculi is of an immature form (Urist, 1964).

Whewellite calculus

P was detected in the nucleus in addition to Ca. As it is undeniable that the moiety of the detected Ca originates from whewellite, it follows that the nucleus contains phosphate in addition to whewellite.

Cystine calculi

S was detected in cystine calculi as expected, but P and Ca also were detected. This fact may indicate that a cystine calculus is not always composed of a single substance.

As a consequence of these findings, it becomes clear that an energy dispersive type X-ray microanalyzer is far more accurate in the analysis of a small area of a calculus than the X-ray diffraction method. The presence of light elements is easily detected, and a scanning image also is obtained at the same time.

Furthermore, a conventional transmission electron microscope produced a far clearer picture than the essential scanning electron microscope. In addition, the use of a computer system presented a clear energy spectrum and the weight fractions of several elements. The technique outlined herein provides exact information on the presence and structure of elements even if a very small sample is used.

The use of an energy dispersive type X-ray microanalyzer together with a computer system should be of great future use in analyzing urinary tract calculi.

ACKNOWLEDGEMENT

The author wishes to thank Dr. Vinci Mizuhira (Department of Cell Biology, Medical Research Institute, Tokyo Medical and Dental University), Dr. Toshimitsu Konjiki and Dr. Hiroshi Kawai (both of the Department of Urology, Nippon Medical School) for their encouragement.

REFREENCES

1) Beischer, D. E.: Analysis of renal calculi by infrared spectroscopy. J. Urol., **73**: 653~659, 1955.
2) Chambers, A., Hodgkinson, A. and Hornung, G.: Electron probe analysis of small urinary tract calculi. Invest. Urol., **9**: 376~384, 1972.
3) Duncumb, P.: EMMA, Combinaison dún microscope électronique et dúne microsonde électronique. Journal de Microscopie, **7**: 581~587, 1968.
4) Hodgkinson, A., Peacock, M. and Nicholson, M.: Quantitative analysis of calcium-containing urinary calculi. Invest. Urol., **6**: 549~561, 1969.

5) La Towsky, L.W.: Qualitative chemical analysis of urinary calculi. J. Urol., **49**: 720～726, 1943.
6) Meyer, A.S., Finlayson, B. and Dubois, L.: Direct observation of urinary stone ultrastructure. Brit. J. Urol., **43**: 154～163, 1971.
7) Mizuhira, V.: Elemental analysis of biological specimens by electron probe X-ray microanalysis. Acta Histochem. Cytochem., **9**: 69～87, 1976.
8) Prien, E.L.: Crystallographic analysis of urinary calculi, A 23-year-survey study. J. Urol., **89**: 917～924, 1963.
9) Prien, E.L. and Frondel, C.: Studies in urolithiasis, 1 The composition of urinary calculi. J. Urol., **57**: 949～994, 1947.
10) Russ, J.C.: X-ray microanalysis in the biological sciences. J. Submicr. Cytol., **6**: 55～79, 1974.
11) Sutor, D.J. and Scheidt, S.: Identification standards for human urinary calculus components using crystallographic methods. Brit. J. Urol., **40**: 22～28, 1968.
12) Sutor, D.J., Wooley, S.E. and Illingworth, J.J.: A geographical and historical survey of the composition of urinary stones. Brit. J. Urol., **46**: 393～407, 1974.
13) Takasaki, E.: An observation on the composition and recurrence of urinary calculi. Urol. Int., **30**: 228～236, 1975.
14) Urist, M.R.: *Recent Advances in Physiology of Calcification*. The Journal of Bone and Joint Surgery, **46**: 889～900, 1964.
15) Westbury, E.J.: Some observations on the quantitative analysis of over 1000 urinary calculi. Brit. J. Urol., **46**: 215～227, 1974.
16) Westbury, E.J. and Omenogor, P.: A quantitative approach to the analysis of renal calculi. Journal of Medical Laboratory Technology, **27**: 462～474, 1970.

(Accepted 1977. 8. 8.)

和文抄録

尿　石　の　元　素　分　析

日本医科大学泌尿器科学教室
剣　木　文　隆

尿石における X 線微少部分の元素分析は，1972年 Chamber らが波長分散型 X線検出器を使って蓚酸塩石の分析を試み，本邦では高崎らが同様な方法で研究報告をしている．今回著者は，エネルギー分散型X線検出器を使って尿石の元素分析をおこない，さらにコンピューター（EDIT 方式）を連結することによって微少領域における元素の定量比を得ることに成功したので報告する．試料は結石患者より摘出した尿石で，X線回折，偏光顕微鏡によりすでに鉱物学的性質が明らかなものから6例を用いた．分析結果は次のとおりである．

1) 3例の apatite 結石のうち1例から Mg が検出された．

2) Whewellite 結石の核からはPが検出された．

3) 2例の cystine 結石からは Ca とPが検出された．

4) 分析された元素はそれぞれの結石においてほとんど同様な分布を示した．

5) apatite 結石の Ca, P の重量比は，理論上と異なった値を示した．